

Imaging Test Setup for the Coded-Mask Gamma-Ray Spectrometer SPI

C. B. Wunderer¹, P. Connell², R. Diehl¹, R. Georgii¹, A. v. Kienlin¹, G. G. Lichti¹, F. Sanchez³,
V. Schönfelder¹, A. Strong¹ and G. Vedrenne⁴

¹Max-Planck-Institut für extraterrestrische Physik, 85470 Garching, Germany

²University of Birmingham, Birmingham, United Kingdom

³Universidad de Valencia, Valencia, Spain

⁴CESR, Toulouse, France

Abstract

ESA's INTERNATIONAL Gamma-Ray Astrophysics Laboratory (INTEGRAL) will be launched in 2002. One of its two main instruments is the Spectrometer SPI. It uses 19 HPGe detectors to observe the sky in the energy range of 20 keV to 8 MeV with a resolution of $\Delta E/E \approx 0.2\%$. Directional information is obtained using a coded mask. The expected angular resolution is about 2° .

The SPI Imaging Test Setup (SPITS) was built at MPE to allow experimental verification of the imaging properties of SPI. SPITS consists of a coded HURA mask and two germanium detectors. The mask is built from 63 opaque tungsten-alloy elements. The two hexagonal Ge-detectors are housed in a common aluminum end cap. They are mounted on an XY-table and can be moved to cover the 19 SPI Ge-detector positions. Mask and Germanium detectors are made of SPI materials, with the exception of some Be parts which have been replaced by thinner Al parts.

The imaging properties of SPITS are being measured with several radioactive sources at a distance of 9 m from the detector plane. We obtain an angular resolution of about 2° at 1.8 MeV and a point-source location capability of SPITS of 15 arcmin at 1.17 MeV. Two sources whose signal/background ratio is 2.7 are reconstructed correctly at 4σ significance level.

I. INTRODUCTION

The INTEGRAL observatory consists of 4 instruments: the imager IBIS will work in the energy range 15 keV – 10 MeV with an angular resolution of $12'$ FWHM and a spectral resolution of $\Delta E/E \approx 6\%$ at 1 MeV, SPI will deliver high resolution spectra ($\Delta E/E \approx 0.2\%$ at 1 MeV) with coarser angular resolution (2° FWHM) in the energy range 20 keV – 8 MeV [1]. In addition to these two main instruments, a small X-ray monitor (JEM-X), and an optical monitoring camera are aboard INTEGRAL to provide multi-wavelength information. All instruments except the optical monitor use tungsten-alloy coded masks to obtain directional information on the incoming radiation.

Although the technique of using coded masks is well known in the X-ray domain (e.g. [2] and references therein), INTEGRAL's instruments will be the first spaceborne detector systems using coded masks up to 10 MeV. INTEGRAL is a follow-up of the SIGMA experiment (1990-1999) [3], with improved sensitivity and an increased energy range. In SPI, for the first time, high purity germanium detectors are

combined with a coded aperture to perform astrophysical observations on a satellite platform. The thickness of the tungsten-alloy mask elements is 30 mm, enough to absorb gamma-rays up to several MeV. Each of the 19 hexagonal Ge crystals has a front area of 27 cm^2 and is 7 cm long.

Studies of the imaging capabilities of SPI were done using GEANT and other simulation tools [4,5,6]. The SPI Imaging Test Setup (SPITS) was built to complement the theoretical studies of SPI imaging performance and to provide the chance to test SPI data-analysis methods on experimental data long before launch. The SPITS results will complement findings from the SPI calibrations which will take place early in 2001.

II. THE SPI IMAGING TEST SETUP

SPITS has a flight instrument (FM)-equivalent coded-aperture mask. Its hexagonal uniformly redundant array (HURA) coding pattern is identical to that of the SPI FM, as

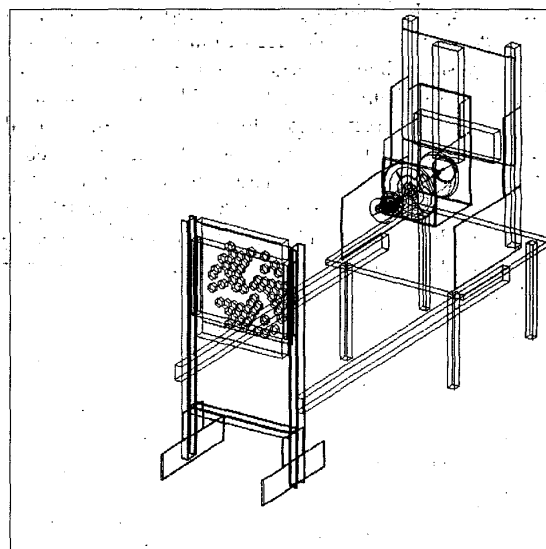
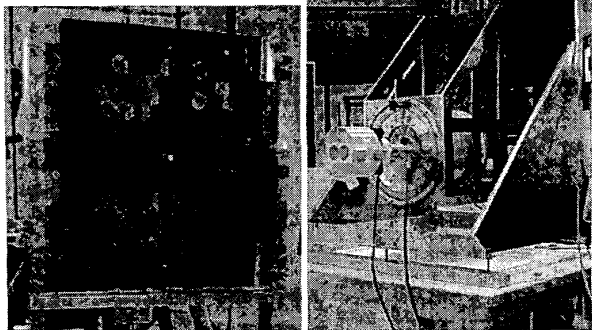


Figure 1: Schematic drawing of the SPI Imaging Test Setup.

are all materials used. The SPITS mask was constructed on the basis of a SPI mask development model which we obtained from the University of Valencia. The only difference between the SPI and SPITS masks is that the honeycomb base



Figures 2 and 3: Photographs of the SPITS mask assembly and the Ge-detectors mounted on the XY-table.

on which the tungsten-alloy elements of the SPITS mask are mounted is rectangular instead of circular.

Instead of SPI's 19 HPGe detectors, for cost reasons SPITS could only be equipped with two. The individual Ge crystals in their hexagonal Al capsules are FM-equivalent. Like the SPI detectors, SPITS' detectors are manufactured by Eurisys [7]. SPITS' two detector capsules are mounted on an Al cold plate (instead of Be for SPI) and placed in a common vacuum end cap made of Al (instead of thicker Be for SPI). Cooling of the SPITS detectors is achieved using liquid nitrogen instead of the SPI cryocooler systems.

The two SPITS detectors can be moved using an XY-table in order to cover all positions of the 19 SPI Ge detectors. A drawing of the SPITS setup is shown in Figure 1, photographs of the mask assembly and the Ge detectors on the XY-table are shown in Figures 2 and 3.

The SPI telescope is equipped with a BGO anticoincidence shield to allow discrimination against charged particles and gamma-rays entering the telescope from the sides. Since background radiation on the ground is at a much lower level, this is not required for SPITS measurements. Also, the SPI telescope has a 5 mm plastic anticoincidence shield between mask and Ge detector plane to improve its 511 keV line sensitivity. This anticoincidence shield is not necessary in a laboratory environment either, so it was replaced by a plexiglass sheet of equivalent thickness to emulate its absorption in the SPITS setup.

III. MEASUREMENTS

For the measurements described here, we used ^{60}Co (1173 keV, 1332 keV) and ^{88}Y (898 keV, 1836 keV) laboratory point sources (diameter of active volume ≈ 1 mm). They were placed in a source holder 9 m from the SPITS detector plane. This setup provides easy source positioning accurate to better than 0.5 arcmin.

The ^{60}Co -source was moved horizontally away from the SPITS instrument axis, initially in steps as small as 2.5'. At each position of the source, an image was measured with 3600 s exposure time for each Ge-detector position. The goal of

these measurements was to determine the point-location accuracy of such a mask-detector combination for a single strong point source at ≈ 1 MeV.

The ^{88}Y -source was moved towards the instrument axis in steps of 0.5°, starting at 3.0° from the instrument axis. Here, the goal was to first determine point-source location accuracy at somewhat larger angles from the instrument axis. Then, data from two such measurements were added to form a composite dataset of two equally strong line sources that are separated by between 0.5° and 3°.

Using ^{152}Eu (several lines, 122 keV to 1528 keV) and ^{88}Y sources at 1.7 m, we measured the photopeak efficiency of the SPITS detectors. With this information we determine how accurately present SPI imaging analysis software reconstructs the intensity of the calibration sources.

IV. IMAGE DECONVOLUTION

For SPI image analysis, two methods are foreseen: (1) *spiskymax* [8], a program based on the maximum-entropy method; this method simultaneously determines the intensity in each sky pixel through an entropy-constrained algorithm, and can be used for point sources and diffuse emission. (2) *spiros* [9], an algorithm that iteratively removes point sources from the image as it determines their location and strength using correlation matrices. In this work, we apply only the maximum-entropy method. SPI image deconvolution algorithms use instrument response functions (IRFs) that reflect the response of all 19 detectors to a source of a given energy at any point in the sky. Since this response is different for sources at infinity and at finite distances – the shadow projection of the mask onto the detector plane is not the same – we use IRFs that fit the SPITS source-detector geometry. These IRFs were calculated using a ray-tracing algorithm (while SPI IRFs will be generated using GEANT simulations).

V. FIRST RESULTS

A. SPITS Location Capability for a Single Strong Point Source

To determine SPITS' ability to accurately locate a strong source, we performed measurements with a ^{60}Co source positioned at 0', 2.5', 5', 10', 20', 30', 40', 50', and 60' from the instrument axis.

In order to estimate SPITS' source-location capability independent of image reconstruction, we calculate the normalized χ^2 between two such sets of raw data. The farther the source positions are apart, the larger the difference between the datasets should be. If more than one pair of datasets has the required angular distance between source positions, we show up to three results for χ^2 to demonstrate the range of values. Each dataset has 19 degrees of freedom (19 independent detectors); there is a less-than 0.1% probability that a χ^2 -value larger than 2.31 would result from two datasets measured under identical conditions, provided there are no systematic differences. χ^2 -values calculated for the 1173 keV and 1332 keV lines of ^{60}Co are shown in Table 1. For

comparison, results from the same χ^2 calculation are shown for the 1461 keV line from natural ^{40}K , a radioactive isotope which is roughly isotropic in the laboratory environment.

Table 1

Normalized χ^2 from comparison of two datasets taken with a single strong ^{60}Co source at different positions; 1461 keV line from natural ^{40}K shown for comparison.

Angular distance [arcmin]	Normalized χ^2 from binned data		
	1173 keV	1332 keV	1461 keV
2.5	5.16	3.22	2.38
2.5	3.17	3.62	1.22
5.0	7.74	8.87	2.31
5.0	8.24	6.03	1.39
5.0	5.87	9.03	0.71
7.5	17.84	16.12	1.15
10.0	28.15	26.16	1.88
10.0	29.81	23.50	1.39
15.0	63.64	49.52	1.07
20.0	92.67	84.25	1.06

Assuming that a χ^2 -value above 15 indicates separability of source locations, the determination of source locations to 7.5 or 10 arcmin seems feasible for single strong sources in a virtually background-free environment.

Next, we deconvolved images for each source position using *spiskymax*. Figure 4 shows a composite image of the results. The dark crosses along the white dashed line mark the true source position in each image.

In an attempt to quantify the deviation of the source position in the image from the real source position, we fit a two-dimensional gaussian to each individual image and calculated the distance from the maximum of the gaussian to the true source position. This deviation was less than 15 arcmin for the sources at 0' to 40'. For the same positions, the width (σ) of the gaussian was between 10 and 20 arcmin. For 50' and 60', the maximum of the reconstructed image is too close to the border of the image for the fit to converge properly. Judging from this, for sources close to the instrument axis a location capability of about 20 arcmin seems feasible with SPI and *spiskymax*.

B. SPITS Angular Resolution

A second goal of SPITS is to determine the angular resolution of such an instrument, i.e. the capability to separate and correctly locate two sources that are close to each other.

We used the ^{88}Y data in the 1836 keV line for this task. As mentioned before, we added data from two measurements with our ~ 3 MBq ^{88}Y source at different positions to obtain a dataset with two ^{88}Y sources. Since ^{88}Y count rates at the detectors are low in this measurement geometry, adding the datasets is legitimate because effects from coincidence are negligible.

We tested several combinations of source positions with angular distances between 1.5° and 2.5°. Figures 5 through 7 show three cases, pixel size in each image is $0.1^\circ \times 0.1^\circ$. Note

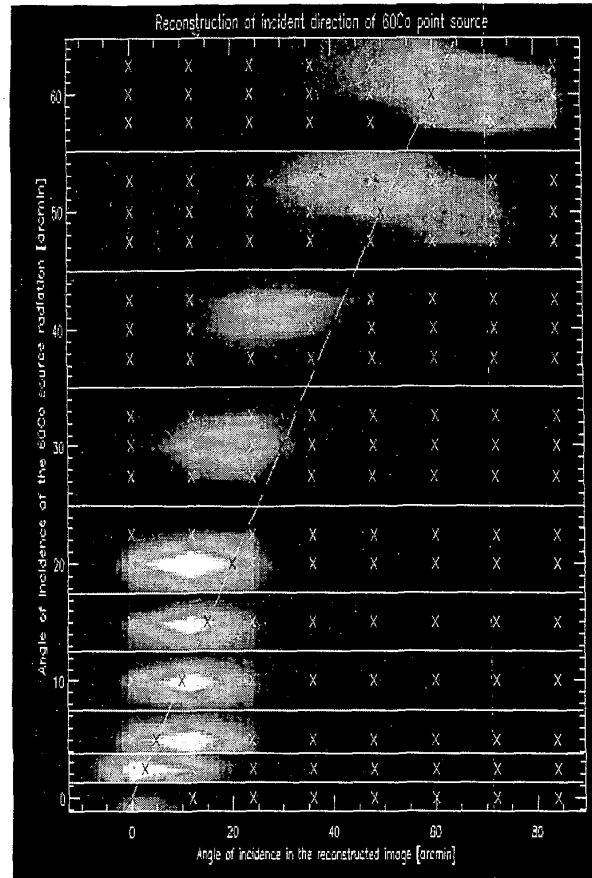


Figure 4: Composite of the reconstructed images of a ^{60}Co source at 0 to 60 arcmin from the instrument axis, source at 9 m. Reconstruction in the 1173 keV line performed using *spiskymax*. Dark Xs along the white dashed line mark true source positions, white Xs mark the gridpoints of the IRF.

how for sources that are too close to be separated properly the reconstructed image shows a source between the two true source positions (denoted by Xs).

C. Reconstruction of Source Intensities

At 1836 keV, we superimposed measurements from a single 3.7 MBq ^{88}Y source. ^{88}Y has a half-life of only 106.65 days. Since the individual measurements were taken several days apart, the two sources in the images have somewhat different intensities. For the composite image in Figure 7 (2.5° separation), this corresponds to 0.255 ± 0.008 photons/(cm² s) for the source at (0.5°, 0.867°) and 0.222 ± 0.007 photons/(cm² s) for the source at (1.75°, 3.03°). (The uncertainty in these fluxes is due to the uncertainty in the calibration of the ^{88}Y source activity).

The *spiskymax* algorithm finds these sources (intensity integrated over a circle with 0.5° radius and compared with a 1.0°-radius circle for background) with a 6.3 σ and 5.1 σ significance, respectively. The reconstructed flux given by our *spiskymax* algorithm must be corrected for an inadequate assumption made in the calculation of the IRFs, namely that

any gamma-ray interacting in a Ge-detector is depositing all its energy there, i.e. contributing to the photopeak. In reality, about 78 % of the 1836 keV photons interact at least once in 7 cm of Ge, while the measured photopeak efficiency of our Ge detectors at 1836 keV is 12.6 ± 1.4 %. If we correct for this, we obtain fluxes of 0.22 ± 0.05 photons/(cm² s) for the source at (0.5°, 0.867°) and 0.17 ± 0.05 photons/(cm² s) for the source at (1.75°, 3.03°). Within error bars, this is in agreement with the fluxes from the calibration source given above.

D. Adding Background to SPITS Data

Up to this point, we used virtually background-free data for our analysis. Since the measurements were performed in a laboratory environment with fairly strong calibration sources, background levels were low. Furthermore, individual lines in the spectra were fitted with gaussians and only the resulting peak areas were fed to *spiskymax* for analysis.

Here, we took the measurement shown in Figure 5 (two ⁸⁸Y sources) and compared results for the 1836 keV line obtained by (1) using the gaussian-fitted data (Figure 7), (2) using all counts in an energy bin $\pm 3\sigma$ wide around the line energy and adding additional background noise to the data (poisson-distributed around 10^3 counts per detector), and (3) again using binned data and adding poisson-distributed background at the level of 10^5 counts per detector. The reconstructed images for cases (2) and (3) are shown in Figures 8 and 9, respectively. The images show $12^\circ \times 12^\circ$ of the ‘sky’, a larger section than Figures 3 to 5, to include artifacts that increase with increasing background levels. Table 2 summarizes the results of the analysis; flux values are determined here from an 1° radius around the true source position.

Table 2
Results from the reconstruction in the 1836 keV line of two ⁸⁸Y point sources, 2.5° apart, with background added to the data.

	Gaussian fit	Background 10 ³ cts/det.	Background 10 ⁵ cts/det.
signal / background.		2.65	0.0265
σ (0.5°, 0.9°) source	7.9	4.5	2.8
σ (1.8°, 3.0°) source	4.2	3.8	1.7
true flux of source at (0.5°, 0.87°):	0.255 ± 0.008 [phot/(cm ² s)]		
reconstructed flux [phot/(cm ² s)]	0.21 ± 0.04	0.21 ± 0.06	0.17 ± 0.07
true flux of source at (1.75°, 3.03°):	0.222 ± 0.007 [phot/(cm ² s)]		
reconstructed flux [phot/(cm ² s)]	0.18 ± 0.05	0.18 ± 0.06	0.11 ± 0.07

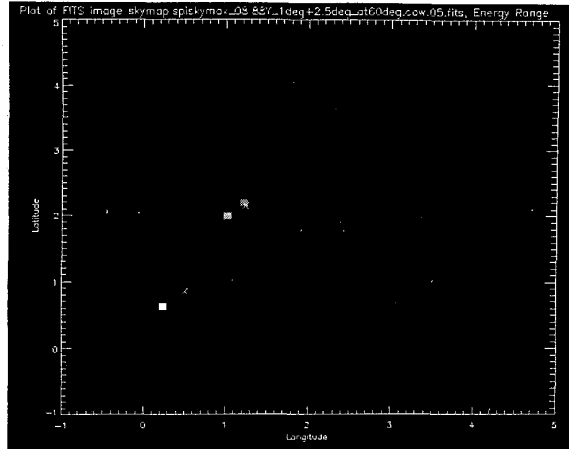


Figure 5: Reconstruction in the 1836 keV line of two ⁸⁸Y point sources at (0.5°, 0.867°) and (1.25°, 2.16°), 1.5° apart.

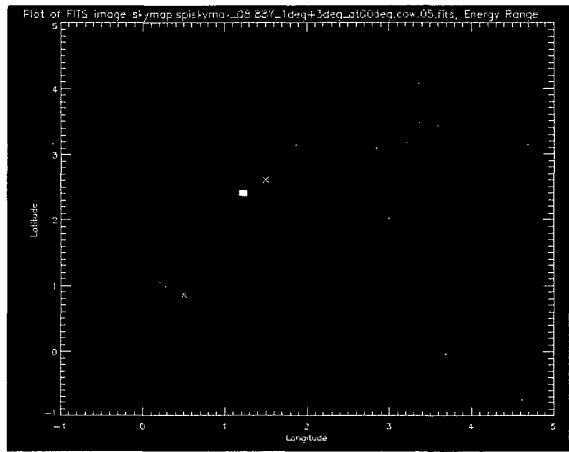


Figure 6: Reconstruction in the 1836 keV line of two ⁸⁸Y point sources at (0.5°, 0.867°) and (1.5°, 2.60°), 2.0° apart.

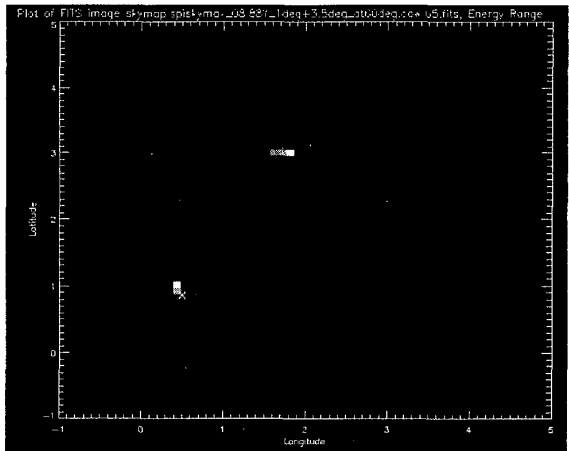


Figure 7: Reconstruction in the 1836 keV line of two ⁸⁸Y point sources at (0.5°, 0.87°) and (1.75°, 3.03°), 2.5° apart.

VI. SUMMARY AND PLANS FOR THE FUTURE

We have demonstrated for the SPITS setup together with the *spiskymax* image-reconstruction algorithm that it can separate and correctly locate and determine the intensity of two point sources in one image. Results from the χ^2 -comparison of raw data suggest that it should be feasible to determine the location of a single strong point source at 1 MeV close to the line of sight of the instrument to $\sim 10'$, while the positions of the source in the images reconstructed from the same data are correct within $15'$. This analysis has been performed with strong point sources in a virtually background-free environment, additional tests with higher background levels remain to be performed.

At 1836 keV, a line energy selected for these test because of its proximity to the astrophysically interesting 1809 keV line from ^{26}Al , SPITS is able to correctly separate sources 2° and more apart. For angular distances of 1.5° and below, ghost images appear between the true source positions. When adding poisson-distributed background to the image data, we obtain good reconstruction of image positions and intensities for signal-to-background levels of 2.7 (significance 3.8σ and 4.5σ , flux within 1σ) and marginal detection at signal-to-background levels of 0.027 (significance 2.8σ and 1.7σ , flux within 2σ).

The next steps with SPITS will include the determination of point-source location capabilities and angular resolution at several gamma-ray energies between 60 keV and 1.8 MeV. We hope to be able to use an accelerator to extend the range of energies up to 8 MeV to cover the full nominal energy range of SPI.

In addition, we will use laboratory sources to simulate extended emission and determine how well SPITS can image such diffuse sources.

VII. REFERENCES

- [1] P. Mandrou et al, "The INTEGRAL Spectrometer SPI," *Proc. 2nd INTEGRAL Workshop*, pp.591-598, 1996.
- [2] M. Badiali et al., "Hard X-ray imaging with a rotating wide field coded mask telescope," *Astron. Astrophys.*, vol. 151, pp.259-263, 1985.
- [3] J. Paul et al., "SIGMA: The hard X-ray and soft gamma-ray telescope on board the GRANAT space observatory," *Adv. Space Res.*, vol. 11, no. 8, pp. 289-302, 1991.
- [4] G. K. Skinner et al., "The spectral line imaging capabilities of the SPI germanium spectrometer on INTEGRAL," *Proc. 4th Compton Symposium vol2*, pp. 1544-1548, 1997.
- [5] P. Connell, "Imaging and Spectral Reconstruction for the INTEGRAL Spectrometer (SPI)," *Proc. 3rd INTEGRAL Workshop*, vol. 2, pp. 397-400, 1999.
- [6] A. W. Strong, "SPI Imaging Prospects for diffuse Galactic Continuum hard X-rays," *Proc. 3rd INTEGRAL Workshop*, vol. 2, pp. 221-224, 1999.
- [7] Germanium detectors are manufactured by Eurisys Mésures, 1 Chemin de la Roseraie, Lingolsheim, France.
- [8] A. W. Strong, "Maximum Entropy Imaging of COMPTEL Data," *Exp. Astronomy*, vol.6, pp 97-102, 1995.
- [9] P. Connell, "Imaging with the INTEGRAL Spectrometer using Constrained Matrix Methods," *Proc. 4th INTEGRAL Workshop*, in print, 2000.

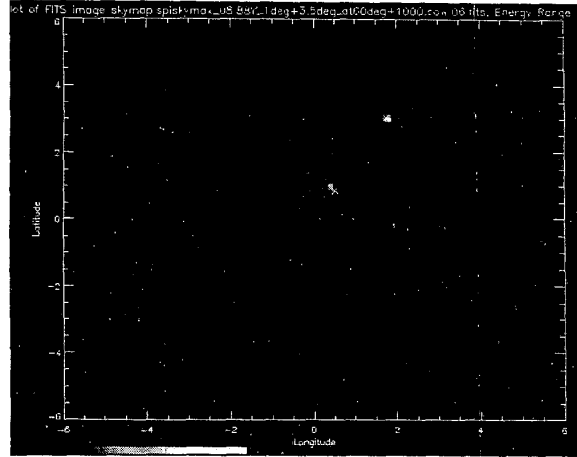


Figure 8: As Figure 5, but poisson-distributed background (10^3 counts/detector) added to the data.

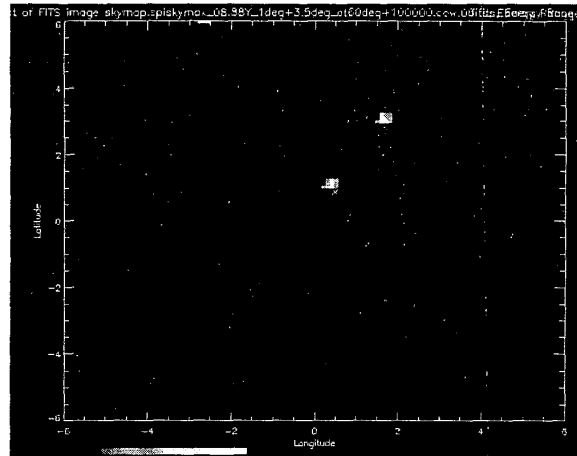


Figure 9: As Figure 5, but poisson-distributed background (10^5 counts/detector) added to the data.